Simulation of rock-breaking process of polycrystalline diamond compact bit under circumferential impact torque

Meiqiu Li*, Ziyu Yang, Jiawen Li, Sizhu Zhou

School of Mechanical Engineering Yangtze University, Jingzhou 434023, China
limeiqiu@sina.com

ABSTRACT. *Stick-slip vibration is commonplace in the drilling of polycrystalline diamond compact (PDC) bit, which leads to early bit failure, low drilling efficiency and high drilling cost. Inspired by the application of torsional impactor, this paper establishes a nonlinear dynamic 3D numerical simulation model, in which the Drucker-Prager criterion is taken as the yield criterion of the rock. Then, the model was applied to simulate the dynamic rock-breaking process of the PDC bit under circumferential torque impactor. The results show that the stick-slip vibration was basically eliminated under the torque impactor, and the rate of penetration (ROP) increased by three times. This means the application of circumferential torque impactor to PDC bit can reduce the stick-slip vibration and enhance the ROP. The research findings provide a theoretical guidance on the application of torsional impactor on PDC bit.*

RÉSUMÉ. *La vibration de stick-slip est un point commun dans le forages au diamant synthétique polycristallin (PDC en anglais), ce qui entraîne au niveau de forage une défaillance précoce, une faible efficacité et un coût élevé. Inspiré par l'application de l'impacteur de torsion, cet article établit un modèle de simulation numérique 3D dynamique non linéaire dans lequel le critère de Drucker-Prager est pris comme critère de rendement de la roche. Ensuite, le modèle a été appliqué pour simuler le processus dynamique de déformation du forages au diamant synthétique polycristallin sous un couple d'impact circonférentiel. Les résultats montrent que la vibration de stick-slip a été pratiquement éliminée sous le couple d'impact et que le taux de pénétration (ROP en anglais) a été multiplié par trois. Cela signifie que l'application du couple d'impact circonférentiel au forages au diamant synthétique polycristallin peut réduire la vibration du stick-slip et améliorer le taux de pénétration. Les résultats de la recherche fournissent des indications théoriques sur l'application de l'impacteur de torsion sur le forages au diamant synthétique polycristallin.*

KEYWORDS: *torsional impactor, polycrystalline diamond compact (PDC) bit, stick-slip vibration, rock-breaking simulation.*

MOTS-CLÉS: *impacteur de torsion, forages au diamant synthétique polycristallin, vibration de stick-slip, simulation de déformation de la roche.*

DOI:10.3166/ACSM.41.299-311

1. Introduction

With the development of the oil industry, more and more deep and ultra-deep wells have been drilled and completed. However, the increasing well depth is accompanied with the growth in the hardness and ductility of rock stratum, leading to poor drillability, low rate of penetration (ROP) and undesirable drilling efficiency. The low efficiency can be partially attributed to the stick-slip vibration at the drill bit. The stick-slip vibration refers to the stick and slip of the drill bit when the angular speed of the bit reduces to zero before the cumulative torque is sufficient to drive the bit rotation again.

The angular speed of the drill bit is usually periodic because the drill string is released and distorted in a periodic manner. In the course of drilling, the drill string exerts a torque on the drill bit. Sufficient torque can break the rock through the rotation of the polycrystalline diamond compact (PDC) bit. Additional torque may occur on the drill bit due to the extra static friction force between the drill string and the well hole and the residual axial displacement of the stuck drill bit. Moreover, the resistance torque on the drill bit increases with the rock strength when the bit cuts through hard rocks.

The application of near-bit torsional impactor is a good way to reduce the stick-slip vibration (Lu *et al.*, 2015; Deen *et al.*, 2011). The impactor can provide a stable and frequent circumferential torque impactor to the drill bit. In this way, less torque will accumulate over time, and thus mitigate the stick-slip vibration. This approach has been adopted in many Chinese oil fields. After applying torsional impactor, the ROP in 3,458.6m~3,678.5m increased by 2.72 times in Qican 1# well, the mean footage grew by 122.38% in φ215.9mm borehole of Yuanba oil field, and the ROP in 3,598m~3,834m rose by 159.14 % to 2.41m/h in Yumengqingxi Q2 66#well (Zhang and Ma, 2012).

None of the existing studies on rock-breaking simulations manages to thoroughly disclose the effects of torsional impactor on drilling (Zhu *et al.*, 2012; Xu, 2015; Li, 2014; Yang *et al.*, 2014). Without considering the influence of the drill string, the previous finite-element models (FEMs) fail to yield close-to-reality simulation results. What is worse, the simulation accuracy is severely affected by the selection of rock material and the determination of the failure conditions.

In light of elastic plastic mechanics and rock mechanics, this paper establishes a nonlinear dynamic 3D numerical simulation model, in which the Drucker-Prager criterion is taken as the yield criterion of the rock. Then, the model was applied to simulate the dynamic rock-breaking process of the PDC bit under circumferential torque impactor.

2. Theoretical analysis

Our FEM consists of a drill string, a PDC bit and a rock mass. The drill string is threaded with the PDC bit, which is in contact with the rock mass. During drilling, the PDC bit breaks the rock mass under the drilling pressure and circumferential

torque. To ensure grid quality and reduce computing time, the structures of all elements to be simulated were simplified properly.

The following assumptions were put forward before the modelling:

(1) The tension of the drill string and the angular speed of the drill bit are constant (See ① in Figure 1).

(2) The drill string is simplified into a spring with certain stiffness (See ② in Figure 1).

(3) The lateral motion of the drill bit is so small as negligible.

As shown in Figure 1, the FEM on the bit mechanics was established in reference to the stick-slip vibration of drag bits using a drill string with a velocity-weakening bit–rock interface (Brett, 1992; Palmov *et al.*, 1995; Challamel, 2000; Tucker and Wang, 1999) and the elastic contact normal to the frictional interface (Martins *et al.*, 1990; Twozydlo *et al.*, 1994; Richard and Detournay, 2000; Tolstoi, 1967).

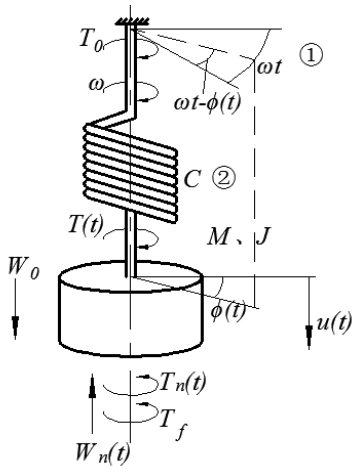

Figure 1. The dynamic model of the borehole assembly (BHA)

Taking the drilling as a continuous process, the forces of the drill string and the drill bit were analyzed in a short period of time, and the kinematic relationship between the rotation angle and vertical position of the drill bit was determined. Then, the differential equation of circumferential motion can be obtained as:

$$C\left[\omega t-\phi(t)\right]=T_s(t)+J\frac{d^2\phi(t)}{dt^2} \tag{1}$$

The differential equations of axial motion can be expressed as:

$$M\frac{d^2u(t)}{dt^2} = W_0 - W_n(t) \tag{2}$$

where C is the torsional rigidity of the drill string; J is the moment of inertia of the BHA; $\phi(t)$ is the rotation angle of the drill bit at time t; ω is the angular speed provided by the drill rig; $T_s(t)$ is the instantaneous torque of the drill bit; $u(t)$ is the axial position of the drill bit at time t; M is the quality of the BHA; W_0 is the stable weight on bit (WOB); $W_n(t)$ is the rock-breaking resistance in the axial direction.

In addition to the torque transferred by the drill string, the drilling process is accompanied with the instantaneous torque $T(t)$ transmitted by the torsional impactor, the resistance torque T_n resulted from rock-breaking, the frictional resistance torque T_f from the rock's interaction with drill string and PDC cutting teeth. Among them, the instantaneous torque can be expressed as:

$$T_s(t) = -T(t) + T_n(t) + T_f \tag{3}$$

The effective moment of inertia of the drill string can be approximated as:

$$J = \frac{\rho I_1 L_1}{3} + \rho I_2 L_2 \tag{4}$$

$$I_1 = \frac{\pi(D_1^4 - d_1^4)}{32} \qquad I_2 = \frac{\pi(D_2^4 - d_2^4)}{32} \tag{5}$$

where ρ is the density of the drilling string; I_1 and I_2 are the polar moment of inertias of the drill pipe and the drill collar, respectively; L_1 and L_2 are the lengths of the drill pipe and the drill collar, respectively; D_1 and d_1 are the outer diameter and inner diameter of the drill pipe, respectively; $D_2$and d_2 are the outer diameter and inner diameter of the drill collar, respectively. Then, the torsional rigidity C of the drill string can be expressed as

$$C = \frac{GI_1}{L_1} \tag{6}$$

where G is the shear modulus of the drill string.

3. Finite-element analysis

3.1. The FEM

Considering the rock-breaking process, the drill string was simplified into a spring with certain torsional stiffness, which is connected to the upper surface of the PDC bit. Besides, the moment of inertia was applied to the spring before simulating

the periodic torsion and release of the drill string.

Table 1 lists the parameters of the drill string for an oilfield operation. These parameters were adopted to calculate the moment of inertia and torsional stiffness of the spring in the FEM. The drill bit was simulated based on a six-blade PDC bit (diameter: 244mm), in which the cutter is distributed evenly on each blade. The bit blades and the bit body were treated as a whole, while the other parts (e.g. inlet, outlet, connectors and chamfers) with little impact on the structure were ignored. The wear of the blades was also neglected because the simulation focuses on the breaking of the rock mass. Viewed as a rigid body, the drill bit was allowed to move freely except along or around the Y-axis. The rock mass was simulated as a cylinder (radius R: 250mm; height H: 200mm). The rock material is a strain-hardening, user-defined material of Drucker-Prager constitutive model. The rock parameters were taken from sandstone and granite (Table 2). The entire FEM is presented in Figure 2 below.

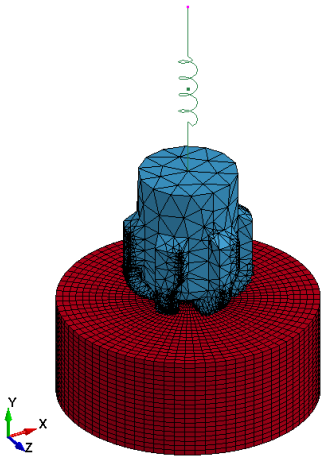

Figure 2. Rock-breaking model of the PDC bit

Table 1. Spring parameters

Torsional rigidity (N·mm/rad)	5×10^{5}	Moment of inertia (t/mm^2)	8.414×10^{4}

Table 2. Rock parameters

Density (t/mm^3)	2.8×10^{-9}	Modulus of elasticity (MPa)	43080
Poisson's ratio	0.19	Rock cohesion (MPa)	110
Internal friction angle (°)	42.95°	Plastic hardening parameter (MPa)	1000

3.2. User-defined material

The strain relationship varies with the well depths under the different confining pressures in rock-breaking. Therefore, the rock material should be selected in light of the specific conditions. Here, the rock material is the rock mass at about 4,400m underground. Thus, the confining pressure can be calculated as (Sun, 2010):

$$p_z = 10^{-6} \rho g z \tag{7}$$

where p_z is the confining pressure (MPa); ρ is the mean density of the overlying stratum (2.2×10-9t/mm^3); g is the gravitational acceleration (9.8m/s^2); z is the buried depth of the rock mass (4,400m). The confining pressure p_z calculated from these parameters was presented in the unit of MPa.

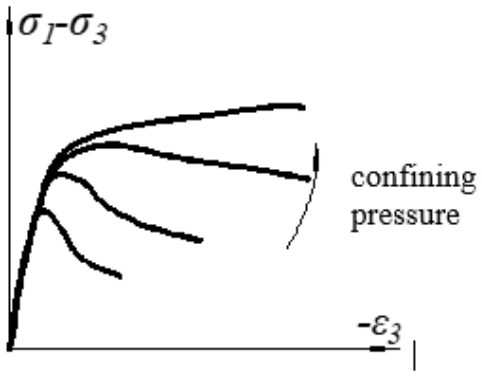

Figure 3. Rock strength under different confining pressures

Figure 3 shows the rock strength under different confining pressures. It can be seen from the figure that the rock mass exhibited a linear hardening trend upon entering the yield phase, and the strain softening ceased to exist. Then, the author prepared a Drucker-Prager constitutive model for the rock mass according to the operating conditions. It is assumed that the rock mass has no defect, the rock softening is negligible and the units are invalid when the plastic strain reach a pre-set value. Besides, the rock mass was assumed to undergo two phases, namely, the elastic phase and the plastic phase. Whether the rock mass will enter the plastic phase and its mechanical properties in this phase are determined by the yield criterion, the isotropic reinforcement criterion and the associated flow pattern.

The user-defined rock material was subjected to a uniaxial compression test and the stress-strain curve was plotted (Figure 4). It can be seen from the curve that the material is suitable for simulation.

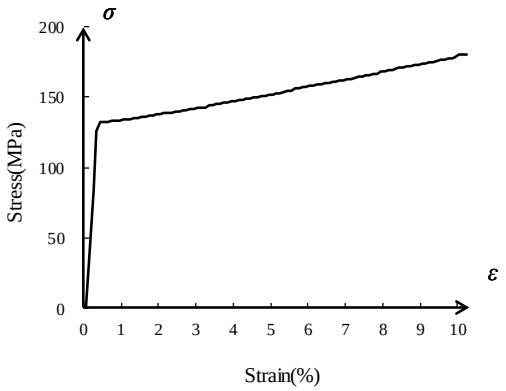

Figure 4. Stress-strain curve of the uniaxial compression test

3.3. Contact and constraint of the FEM

In the drilling process, the PDC bit is always in contact with the rock mass until the latter is broken. Without considering the effect of the rock mass on drilling, the bit-rock contact was regarded as an ESTS. Any rock unit failing to reach the failure condition was removed immediately, while the remaining units were still calculated. Since the rock mass has not boundary in the stratum, the outer surfaces of the rock mass were considered as bound-free except the upper surface. To eliminate the impact of dilatational and shear waves on the results, the surfaces were treated as non-reflecting boundaries.

3.4. Load of the FEM

During drilling, the rotation of the drill bit is driven by the drill string above it, which is in turn driven by the drilling rig. Assuming that the pulling force and rotation speed of the rig are constant, a node of the spring element was selected as the mounting point to simulate the rotation of the drilling rig. In this way, the simulation can cover the entire transfer process of the torque from the rig to the bit. Since it is twisted in contact with the well wall, the drill string was assumed to suffer from a friction torque opposite to the rotational direction of the bit.

Meanwhile, a torsional torque will be generated from the torsional impactor. Taking Reference (Li *et al.*, 2015) for example, the torsional torque was 875Nm and the frequency was 16.5Hz when the inlet pressure of the drilling fluid was 26MPa, and the two parameters increased with the inlet pressure. Several torsional impactors are studied in Reference, whose impact torques were between 650Nm and 1,650Nm and frequencies were between 11Hz and 25Hz. In this paper, the torsional impact torque of 1,000Nm and frequency of 16.67Hz are simulated, without considering the

loss in transmission. To simulate the bit weight, the external load was constant is the Y direction to the drill bit.

4. Simulation results and analysis

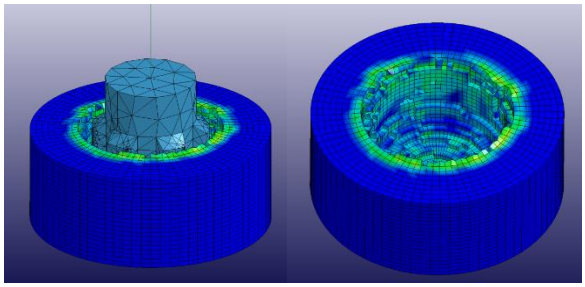

Figure 5. The state of rock-breaking

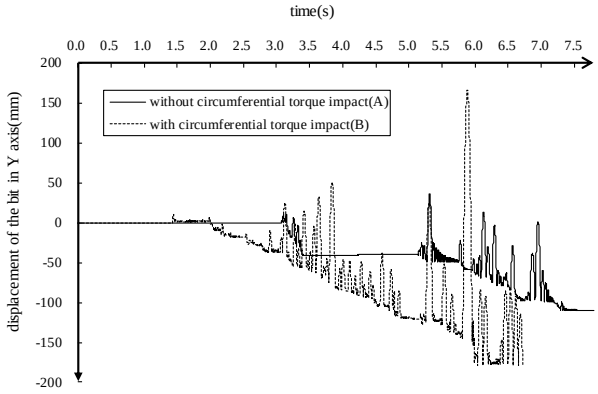

Figure 6. Bit displacement on the Y-axis

According to the simulated rock-breaking state is shown in Figure 5, some rock units disappeared after the drill bit moved downward into contact with the rock mass, indicating that the rock mass is broken. The rock elements on the well wall obeyed a non-uniform distribution, which reflects the discontinuity of the drilling process. The contour of the cumulative plastic strain shows that the rock units near the breaking field had much higher strain than the peripheral units. This means the bit-rock interaction had little impact on the peripheral rock. The bit displacement on the Y-axis is shown in Figure 6 below.

As shown in Figure 6, there was a spring back in Y-axis displacement, which signifies the axial vibration phenomenon in drilling. On Curve A, the bit came into

contact with the rock at t=3s, and exhibited an obvious sticking phenomenon at t=3.45~5s and t=7.24s. On Curve B, however, the bit came into contact with the rock at t=1.88s with no obvious sticking throughout the drilling. In general, curve B is much more continuous than curve A. In addition, the drilling depth was deeper after applying the torque impactor. For instance, at t=5s, the depth without torque impactor was -40.3mm while that with the torque was -119.1mm. This means the torque impactor could accelerate the drilling process.

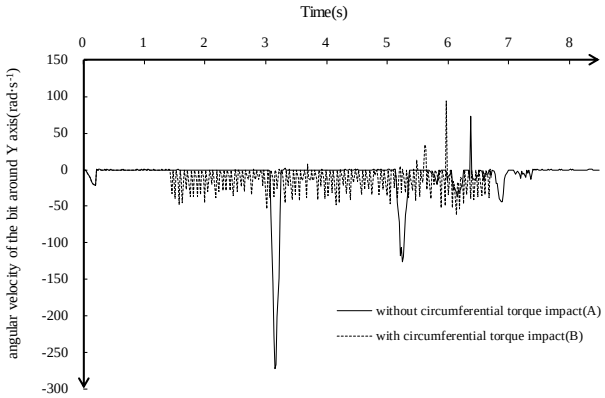

Figure 7. Angular speed of the drill bit around the Y-axis

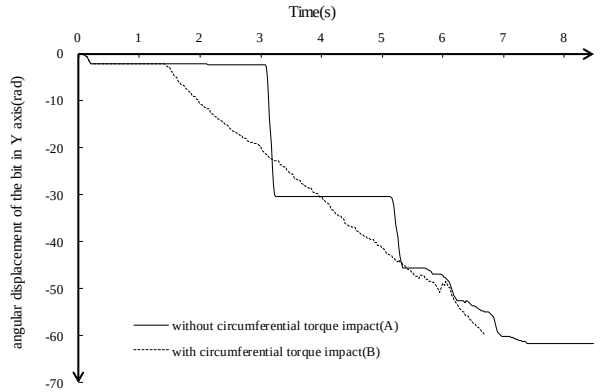

Figure 8. Angular displacement of the drill bit around the Y-axis

On Curve A in Figure 7, the bit was stuck when the angular speed was zero at t=1.5~3s, and slipped off when the speed resumed to 272.3rad/s, an evidence to

obvious stick-slip vibration. By contrast, the angular speed varied gradually between zero and 50rad/s on Curve B, indicating that the stick slip vibration is eliminated.

In Figure 8, the ladder-type Curve A demonstrates obvious abnormalities in the drilling, while the straight Curve B means the drilling was stable and smooth. The results are similar to those on angular speed.

5. Application test

5.1. Lab test

Figure 9. Test device

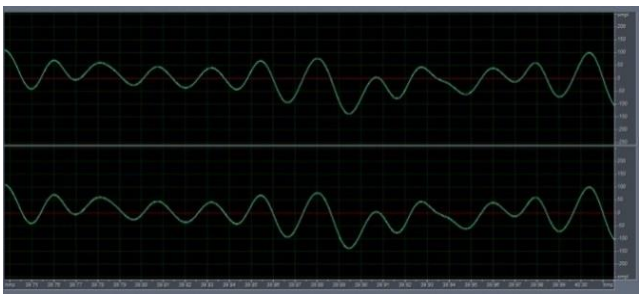

Figure 10. Impact frequency after filtering

A lab test was conducted on a torque impactor (Figure 9), and the impact frequency data were filtered before analysis. It is discovered that the vibration frequency was about 33Hz (Figure 10). According to the working principle of the torsional impactor, the frequency to generate torsional moment is about 16.5Hz, about 990 times per minute. The experimental results show that the test device can produce periodic vibration at high frequency, laying the basis for efficient rock-breaking.

5.2. Field test

Figure 11. Field test

The torque impactor was applied to the drilling of an oil well in a Chinese oilfield. During drilling, the rock mass was so hard that the drill bit could not reach the depth of 1,400m. After pulling out, it is found that the connection between the screw drill and the drill bit became loose. The timely pull-out prevented the bit from falling into the downhole. Then, a torque impactor was installed before carrying out a 60h-long drilling. With the impactor, the drilling of the well was completed successfully, reaching the target layer. The test results show that the torque impactor can improve the drilling efficiency and stability when the rock mass is very hard.

6. Conclusions

This paper sets up an interactive FEM between the PDC bit and the rock mass, and analyzes the effect of circumferential torque impactor on well drilling. The FEM uses a user-defined material, whose mechanical properties were determined by the Drucker-Prager yield criteria and confining pressure. After applying 1,000Nm(16.67Hz) circumferential impact torque, the ROP almost tripled without causing obvious sticking. This means the stick-slip vibration is basically eliminated. Meanwhile, the rotational speed of the drill bit ranged from 0 to 50rad/s, indicating that the bit suffers from no high-speed wear. Then, the torsional impactor was tested in the lab and on an oil field. The test results show that the impactor can produce high-frequency, periodical circumferential impact torque, and improve the ROP and drilling efficiency in hard rock mass. The research findings lay the basis for applying torsional impactor on PDC bit and in other engineering cases.

Acknowledgement

Project supported by PetroChina Innovation Foundation (Grant No. 2015D-5006-0310)

References

Brett J. F. (1992). The genesis of torsional drillstring vibrations. *SPE Drilling Engineering*, Vol. 7, No. 3, pp. 168–174. https://doi.org/10.2118/21943-PA

Challamel N. (2000). Rock destruction effect on the stability of a drilling structure. *Journal of Sound and Vibration*, Vol. 233, No. 2, pp. 235-254. https://doi.org/10.1006/jsvi.1999.2811

Deen C., Wedel R., Nayan A., Mathison S., Hightower G. (2011). Application of a torsional impact hammer to improve drilling efficiency. *Proceedings of the SPE Annual Technical Conference and Exhibition, SPE*. https://doi.org/10.2118/147193-MS

Li H. (2014). Numerical simulation of rock breaking of PDC cutting teeth under torsional impact. *Southwest Petroleum University*.

Li M. Q., Cao Y., Wang Q. J., Li N., Huang T. C. (2015). Dynamics of circumferential torque hydraulic shock generator. *China Petroleum Machinery*, Vol. 43, No. 11, pp. 44-47. https://doi.org/10.16082/j.cnki.issn.1001-4578.2015.11.009

Lu L. L., He D. S., Zhang W. D. (2015). Research and application prospect of torsional impact hammer. *Oil Field Equipment*, pp. 82-85, 2015. https://doi.org/10.3969/j.issn.1001-3842.2015.06.019

Martins J. A. C., Oden J. T., Simo F. M. F. (1990). A study of static and kinetic friction. *International Journal of Engineering Science*, Vol. 28, No.1, pp. 29-92. https://doi.org/10.1016/0020-7225(90)90014-A

Palmov V. A., Brommundt E.,. Belyaev A. K. (1995). Stability analysis of drillstring rotation. *Dynamics and Stability of Systems*, Vol. 10, No. 2, pp. 99-110. https://doi.org/10.1080/02681119508806197

Richard T., Detournay E. (2000). Stick-slip motion in a friction oscillator with normal and tangential mode coupling. *Compte Rendus del'Acade´mie des Sciences*, Vol. 328, No. 9, pp. 671-678. https://doi.org/10.1016/S1620-7742(00)01240-X

Sun Y. H. (2010). Modeling and numerical simulation of fractured low permeability sandstone reservoir. *Tianjin science and technology press*.

Tolstoi D. M. (1967). Significance of the normal degree of freedom and natural normal vibrations in contact friction. *Wear*, Vol. 10, No. 3, pp. 199-213. https://doi.org/10.1016/0043-1648(67)90004-X

Tucker R. W., Wang C. (1999). An integrated model for drill-string dynamics. *Journal of Sound and Vibration*, Vol. 224, No. 1, pp. 123-165. https://doi.org/10.1006/jsvi.1999.2169

Twozydlo W. W., Becker E. B., Oden J. T. (1994). Numerical modeling of friction-induced vibrations and dynamic instabilities. *Applied Mechanics Reviews*, Vol. 47, No. 7, pp. 255–274. https://doi.org/10.1115/1.3111081

Xu Y. K. (2015). The rock-breaking mechanism and experimental study of PDC bits under torsional impact. *Northeast Petroleum University*.

Yang X. L., Song J. W., He S. M., Yu X. L. (2014). Evaluation of parameters for torsional impact to break rock. *Oil Field Equipment*, No. 9, pp. 4-8. https://doi.org/10.3969/j.issn.1001-3482.2014.09.002

Zhang H. W., Ma Y. J. (2012). Analysis and study on application of torkbuster torsional impactor. *Liaoning Chemical Industry*, pp. 841-843. https://doi.org/10.3969/j.issn.1004-0935.2012.08.031

Zhu X. H., Tang L. P., Tong H. (2012). Rock breaking mechanism of a high frequency torsional impact drilling. *Journal of Vibration and Shock*, pp. 75-78. https://doi.org/10.3969/j.issn.1000-3835.2012.20.017